On the Evaluation of the Common-Mode Current Along Twisted-Wire-Pairs

Oussama Gassab[1], Liang Zhou[1], and Wen-Yan Yin[1,2]
[1] Key Lab of Ministry of Education for the Design and EMC of High-Speed Electronic Systems, Shanghai Jiao Tong University, Shanghai 200240, China
[2] Information Science and Electronic Engineering, Zhejiang University, Hangzhou 310058, China
gassab@sjtu.edu.cn, liangzhou@sjtu.edu.cn, and wyyin@zju.edu.cn

***Abstract*—The integral equations describing the common current (CM) along twisted-wire pairs (TWPs) above a ground plane are derived. It is shown that the CM current along TWPs is approximately equal to the one generated by a wire above a ground plane with equivalent radius. In addition, it is verified that the near field radiated by both TWPs and one wire above the ground are also "identical". The analytical results provide a general proof to the CM equivalent circuit that was developed only under engineering guess. Moreover, the obtained results are validated by using the commercial software FEKO and good agreements are obtained.**

***Keywords*—Common mode (CM), Common mode equivalent circuit, field-to-wire coupling, near field, twisted-wire pair (TWP).**

I. Introduction

Transmission line (TL) model was extensively used to predict the response of multi-conductor transmission line (MTL) [1]-[6] under the assumption of electrically small cross-section dimension of the line, the sum of the line currents at any cross-section of the line is zero, and the response of the line is quasi-TEM. However, the sum of the line currents at any cross-section is not always equal to zero if there is a floating terminal i.e., no connection to the ground, connected to any differential line in the MTL cables. Under that reason, the common current (CM), the so called the antenna mode current, is generated along the differential line connected to floating terminals [7]. In the past recent years, different methods were proposed to improve the TL model so as to obtain the exact CM current along its line. e.g., in [8], the current induced along a finite wire above the ground irradiated by plane wave electromagnetic was predicted by using perturbation method, and the telegrapher's equations were extended at very high frequencies to include radiations effects of an infinite line above the ground by Nitsch and Tkachenko in [9]. More recently, their method was extended to be applicable to MTL cables with finite length [10].

To evaluate the antenna mode current along two parallel wires in free space, Vukicevi et al [11] have developed integral equations from the scattering theory and it was shown that these integral equations can be reduced to a pair of TL-like equations with equivalent line parameters. As consequence, the antenna mode current can be obtained by only solving the TL-like equations. In [12] and [13], it was shown that the CM current induced along the TWP wires can be approximated by using the CM equivalent circuit. However, this is only an engineering guess that was suggested without any mathematical proof. In this paper our purpose is to develop generalized integral equations that help us to predict the CM current induced along TWPs wires as well as its near field.

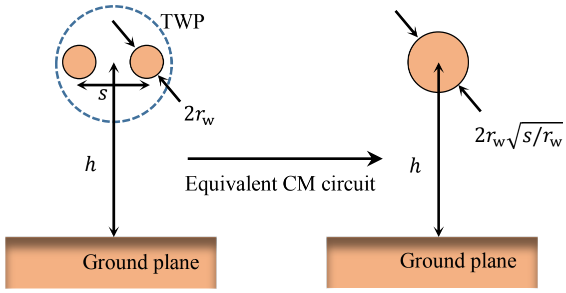

Fig. 1. The equivalent CM circuit of TWP.

II. Mathematical Formulation

In this section, The CM equivalent circuit, proposed in [12] and used in [6] and [13], is proved by using Maxwell's integral equations. The principle of the CM circuit is to replace the TWP by one wire with same height above the ground, Fig. 1, with equivalent radius given as

$$r_{\mathrm{eq,CM}} = r_{\mathrm{w}}\sqrt{s/r_{\mathrm{w}}}\,. \tag{1}$$

Let's suppose a TWP running above ground plane with height h, and it is irradiated by electromagnetic plane wave as shown in Fig. 2. The TWP has twist pitch p, the saparation between the wires is s and wire radius r_{w}. The total length of each wire is $\mathcal{L}$, and they extend along the z-axis with distance $\mathcal{L}_z = \alpha p\mathcal{L}/2\pi$.

A. Derivation of the Integral Equations

By following the same procedures used in [9] and [11]. The scattered field irradiated from the TWP is given as [13]

$$\vec{E}^{\mathrm{sct}} = -j\omega\vec{A} - \vec{\nabla}\Phi \tag{2a}$$

$$\vec{A}(\vec{r}) = \frac{\mu_0}{4\pi}\frac{2\pi}{p\alpha}\int_0^{\mathcal{L}}\sum_{n=1}^{2} I_n(\ell')\left(\vec{n}_{\mathrm{l}_n}(\ell')g_1(\vec{r}-\vec{r}_n') - \widetilde{\vec{n}_{\mathrm{l}_n}}(\ell')g_2\left(\vec{r}-\tilde{\vec{r}}_n'\right)\right)d\ell' \tag{2b}$$

$$\Phi(\vec{r}) = -\frac{1}{\mu_0\epsilon_0 j\omega}\vec{\nabla}\cdot\vec{A} \tag{2c}$$

where $I_n(\ell')$ are the current along the TWP wires, $\vec{A}$ and Φ are the magnetic vector potential and the scalar electric potential, respectively. The vector $\vec{r}_n'$ is the position vector of the source point, for the case of the TWP is given as

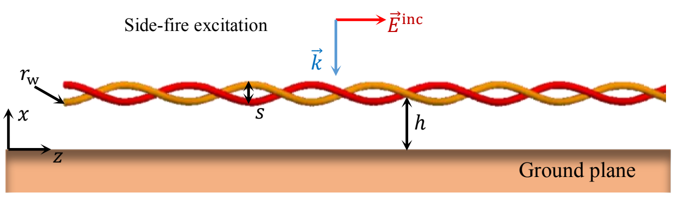

Fig. 2. A TWP above a ground plane and irradiated by a plane wave along the side-fire excitation.

$$\vec{r}_n' = x_n(\ell')\vec{a}_x + y_n(\ell')\vec{a}_y + z_n(\ell')\vec{a}_z \tag{3a}$$

$$x_n(\ell') = h + \frac{s(-1)^{n+1}}{2}\cos(\alpha\ell') \tag{3b}$$

$$y_n(\ell') = \frac{s(-1)^{n+1}}{2}\sin(\alpha\ell') \tag{3c}$$

$$z_n(\ell') = \frac{p\alpha\ell'}{2\pi} \tag{3d}$$

The quantity $\alpha = 1/\left(\left(\frac{s}{2}\right)^2 + \left(\frac{p}{2\pi}\right)^2\right)^{1/2}$ is the rotation parameter of the TWP, the vectors $\vec{n}_{l_n}(\ell')$ and $\widetilde{\vec{n}_{l_n}}(\ell')$ are the unit tangent vector along the TWP real and image wires, respectively, and they are given as

$$\vec{n}_{l_n}(\ell') = \frac{-s\alpha(-1)^{n+1}}{2}\sin(\alpha\ell')\,\vec{a}_x + \frac{s\alpha(-1)^{n+1}}{2}\cos(\alpha\ell')\,\vec{a}_y + \frac{p\alpha}{2\pi}\vec{a}_z \tag{4a}$$

$$\widetilde{\vec{n}_{l_n}}(\ell') = \frac{s\alpha(-1)^{n+1}}{2}\sin(\alpha\ell')\,\vec{a}_x + \frac{s\alpha(-1)^{n+1}}{2}\cos(\alpha\ell')\,\vec{a}_y + \frac{p\alpha}{2\pi}\vec{a}_z \tag{4b}$$

The functions $g_1(\vec{r} - \vec{r}_n')$ and $g_2(\vec{r} - \tilde{\vec{r}}_n')$ are the green functions of the real TWP wires and their images with respect to the ground, respectively, and they are given by [13]

$$\underbrace{g_1(\vec{r} - \vec{r}_n') = \frac{e^{-jk\|\vec{r}-\vec{r}_n'\|}}{\|\vec{r}-\vec{r}_n'\|}}_{\text{real TWP wires}},\ \underbrace{g_2(\vec{r} - \tilde{\vec{r}}_n') = \frac{e^{-jk\|\vec{r}-\tilde{\vec{r}}_n'\|}}{\|\vec{r}-\tilde{\vec{r}}_n'\|}}_{\text{mirrored wires}} \tag{5a,b}$$

where $k = 2\pi f/c$ is the wavenumber in which f is the frequency and c is the speed of light in the free space. Note that $\tilde{\vec{r}}_n'$ is the image of the vector $\vec{r}_n'$ with respect to the ground plane, finally $\vec{r} = x\vec{a}_x + y\vec{a}_y + z\vec{a}_z$ is the position vector where the scattered field is measured (observed).

B. The CM Current Along the TWPs

Now let's derive the CM current along the TWPs wires by using the integral equations (2a-b). Since the wires are assumed to be perfectly conducting, the total tangential electric field should equal to zero. Under the assumption of the thin wire approximation, this condition can be expressed as

$$\vec{E}\cdot\vec{n}_{l_m}(\ell') = \left(\vec{E}^{\rm sct} + \vec{E}^{\rm inc}\right)\cdot\vec{n}_{l_m}(\ell') = 0 \tag{6}$$

where $m = 1$ or 2 for wire 1 or 2, respectively.

We should indicate that $\vec{n}_{l_n}(\ell')\cdot\vec{n}_{l_m}(\ell)$ and $\widetilde{\vec{n}_{l_n}}(\ell')\cdot\vec{n}_{l_m}(\ell)$ have the following expressions

$$\vec{n}_{l_n}(\ell')\cdot\vec{n}_{l_m}(\ell) = \frac{s^2\alpha(-1)^{n+m}}{4}\cos\alpha(\ell-\ell') + \left(\frac{p\alpha}{2\pi}\right)^2 \tag{7a}$$

$$\widetilde{\vec{n}_{l_n}}(\ell')\cdot\vec{n}_{l_m}(\ell) = \frac{s^2\alpha(-1)^{n+m}}{4}\cos\alpha(\ell+\ell') + \left(\frac{p\alpha}{2\pi}\right)^2 \tag{7b}$$

By inserting (7a) and (7b) into (2b) we get the following

$$\vec{A}(\vec{r}_m)\cdot\vec{n}_{l_m}(\ell) = \frac{\mu_0}{4\pi}\frac{2\pi}{p\alpha}\int_0^{\mathcal{L}}\sum_{n=1}^{2} I_n(\ell')\left\{\frac{s^2\alpha(-1)^{n+m}}{4}\left(\cos\alpha(\ell-\ell')\,g_1(\vec{r}_m - \vec{r}_n') - \cos\alpha(\ell+\ell')\,g_2(\vec{r}_m - \tilde{\vec{r}}_n')\right) + \left(\frac{p\alpha}{2\pi}\right)^2\left(g_1(\vec{r}_m - \vec{r}_n') - g_2(\vec{r}_m - \tilde{\vec{r}}_n')\right)\right\}\mathrm{d}\ell' \tag{8}$$

Note that $g_1(\vec{r}_m - \vec{r}_n') = g_1(\vec{r}_n - \vec{r}_m')$ and by taking the following approximation for the condition $h \gg s$, we have

$$g_2(\vec{r}_m - \tilde{\vec{r}}_n') \cong g_2(\ell - \ell') = \frac{\exp\left(-jk\sqrt{(2h)^2 + \left(\frac{p\alpha}{2\pi}\right)^2(\ell-\ell')^2}\right)}{\sqrt{(2h)^2 + \left(\frac{p\alpha}{2\pi}\right)^2(\ell-\ell')^2}} \tag{9}$$

By using the above results, the following equation is obtained

$$\vec{A}(\vec{r}_1)\cdot\vec{n}_{l_1}(\ell) + \vec{A}(\vec{r}_2)\cdot\vec{n}_{l_2}(\ell) = \frac{\mu_0}{4\pi}\frac{2\pi}{p\alpha}\int_0^{\mathcal{L}}\frac{s^2\alpha}{4}\left(g_1(\vec{r}_1 - \vec{r}_1') - g_1(\vec{r}_1 - \vec{r}_2')\right)I_{\rm CM}(\ell')\mathrm{d}\ell' + \frac{\mu_0}{4\pi}\frac{2\pi}{p\alpha}\int_0^{\mathcal{L}}\left(\frac{p\alpha}{2\pi}\right)^2\left(g_1(\vec{r}_1 - \vec{r}_1') + g_1(\vec{r}_1 - \vec{r}_2') - 2g_2(\ell-\ell')\right)I_{\rm CM}(\ell')\mathrm{d}\ell' \tag{10}$$

where $I_1(\ell') + I_2(\ell') = I_{\rm CM}(\ell')$

By following the same method performed in [11] for the CM case, and summing the equations resulted from (6) for $(m = 1,2)$ and with the equation (2a), the following equation is obtained

$$\vec{\nabla}\Phi(\vec{r}_1)\cdot\vec{n}_{l_1}(\ell) + \vec{\nabla}\Phi(\vec{r}_2)\cdot\vec{n}_{l_2}(\ell) + j\omega\left(\vec{A}(\vec{r}_1)\cdot\vec{n}_{l_1}(\ell) + \vec{A}(\vec{r}_2)\cdot\vec{n}_{l_2}(\ell)\right) = \vec{E}^{\rm inc}(\vec{r}_1)\cdot\vec{n}_{l_1}(\ell) + \vec{E}^{\rm inc}(\vec{r}_2)\cdot\vec{n}_{l_2}(\ell) \tag{11}$$

The quantities $g_1(\vec{r}_1 - \vec{r}_1')$ and $g_1(\vec{r}_1 - \vec{r}_2')$ have the following expressions

$$g_1(\vec{r}_1 - \vec{r}_1') = \frac{\exp\left(-jk\sqrt{\frac{s^2}{2}(1-\cos\alpha(\ell-\ell')) + \left(\frac{p\alpha}{2\pi}\right)^2(\ell-\ell')^2}\right)}{\sqrt{\frac{s^2}{2}(1-\cos\alpha(\ell-\ell')) + \left(\frac{p\alpha}{2\pi}\right)^2(\ell-\ell')^2}} \tag{12a}$$

$$g_1(\vec{r}_1 - \vec{r}_2') = \frac{\exp\left(-jk\sqrt{\frac{s^2}{2}(1+\cos\alpha(\ell-\ell')) + \left(\frac{p\alpha}{2\pi}\right)^2(\ell-\ell')^2}\right)}{\sqrt{\frac{s^2}{2}(1+\cos\alpha(\ell-\ell')) + \left(\frac{p\alpha}{2\pi}\right)^2(\ell-\ell')^2}} \tag{12b}$$

Now let's make a comparison between $g(\ell-\ell') = \left(g_1(\vec{r}_1 - \vec{r}_1') + g_1(\vec{r}_1 - \vec{r}_2')\right)/2$ and $g_3(\ell-\ell')$, where $g_3(\ell-\ell')$ is given as

$$g_3(\ell-\ell') = \frac{\exp\left(-jk\sqrt{r_{\rm eq,CM}^2 + \left(\frac{p\alpha}{2\pi}\right)^2(\ell-\ell')^2}\right)}{\sqrt{r_{\rm eq,CM}^2 + \left(\frac{p\alpha}{2\pi}\right)^2(\ell-\ell')^2}} \tag{13}$$

where $r_{\rm eq,CM}$ is given in equation (1)

The results of the comparison are presented in the Fig. 3. It is evident that the green function $g(\ell-\ell')$ and $g_3(\ell-\ell')$ values are "identical". As consequence, it is possible to replace $g(\ell-\ell')$ by $g_3(\ell-\ell')$ in the equation (10).

To see if it is possible to neglect the $\text{term}_1 = (s^2\alpha/4)\left(g_1(\vec{r}_1 - \vec{r}_1') - g_1(\vec{r}_1 - \vec{r}_2')\right)$ with respect to the $\text{term}_2 = (p\alpha/2\pi)^2\left(g_1(\vec{r}_1 - \vec{r}_1') + g_1(\vec{r}_1 - \vec{r}_2') - 2g_2(\ell-\ell')\right)$, we generate Fig. 4.

We can conclude that $\text{term } 1 \ll \text{term } 2$, as fact of that term 1 can be neglected in the equation (10)

In the other hand $\vec{\nabla}\Phi(\vec{r}_1)\cdot\vec{n}_{l_1}(\ell)$ and $\vec{\nabla}\Phi(\vec{r}_2)\cdot\vec{n}_{l_2}(\ell)$ represent the directional derivative of the potential Φ in the direction $\vec{n}_{l_1}(\ell)$ and $\vec{n}_{l_2}(\ell)$, respectively. Since $\vec{r}_1$ and $\vec{r}_2$ are pointing to two points which they are very near to each other's, the following mathematical approximation can be taken

$$\vec{\nabla}\Phi(\vec{r}_1)\cdot\vec{n}_{l_1}(\ell) + \vec{\nabla}\Phi(\vec{r}_2)\cdot\vec{n}_{l_2}(\ell) \cong \vec{\nabla}\Phi\left(\frac{\vec{r}_1+\vec{r}_2}{2}\right)\cdot\left(\vec{n}_{l_1}(\ell) + \vec{n}_{l_2}(\ell)\right) = \vec{\nabla}\Phi\left(\frac{\vec{r}_1+\vec{r}_2}{2}\right)\cdot\left(2\frac{p\alpha}{2\pi}\vec{a}_z\right) \tag{14a}$$

$$\vec{\nabla}\Phi(\vec{r}_1)\cdot\vec{n}_{l_1}(\ell) + \vec{\nabla}\Phi(\vec{r}_2)\cdot\vec{n}_{l_2}(\ell) \cong \frac{\partial\Phi(h,0,z)}{\partial z}2\frac{p\alpha}{2\pi} = 2\frac{\partial\Phi\left(h,0,\frac{p\alpha\ell}{2\pi}\right)}{\partial\ell} \tag{14b}$$

where the CM voltage is defined as [11]

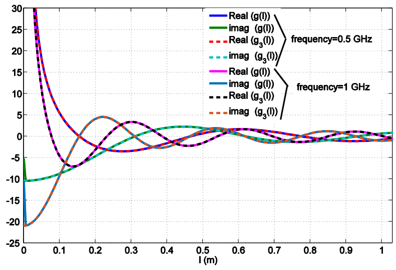

(a)

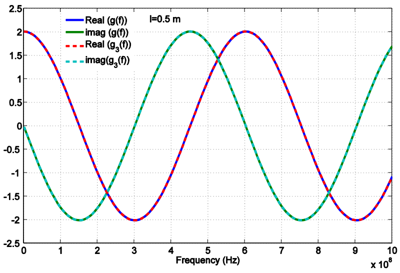

(b)

Fig. 3. The comparison between the green functions $g(\ell-\ell')$ and $g_3(\ell-\ell')$ shows a good agreement.

$$\mathrm{V_{CM}}(\ell)=\frac{\Phi(\vec{r}_1)+\Phi(\vec{r}_2)}{2}\cong\Phi\left(\frac{\vec{r}_1+\vec{r}_2}{2}\right) \tag{15}$$

We perform the same approximation for the expression $\vec{E}^{\mathrm{inc}}(\vec{r}_1)\cdot\vec{n}_{l_1}(\ell)+\vec{E}^{\mathrm{inc}}(\vec{r}_2)\cdot\vec{n}_{l_2}(\ell)$ to get the following

$$\vec{E}^{\mathrm{inc}}(\vec{r}_1)\cdot\vec{n}_{l_1}(\ell)+\vec{E}^{\mathrm{inc}}(\vec{r}_2)\cdot\vec{n}_{l_2}(\ell)\cong 2\frac{p\alpha}{2\pi}E_z^{\mathrm{inc}}\left(h,0,\frac{p\alpha\ell}{2\pi}\right) \tag{16}$$

By inserting (10) and (14)-(16) into (11) and performing the change of variable $z=p\alpha\ell/(2\pi)$, the following equation is obtained

$$\frac{\partial \mathrm{V_{CM}}(h,0,z)}{\partial z}+j\omega\frac{\mu_0}{4\pi}\int_0^{\mathcal{L}_z}\big(g_3(z-z')-g_2(z-z')\big)I_{\mathrm{CM}}(z')\mathrm{d}z'=E_z^{\mathrm{inc}}(h,0,z) \tag{17}$$

The equation (17) has the same form for the CM current along one wire above ground [8]

To derive the second TL-like equation, the same steps are followed. The definition of the CM voltage is given as

$$\mathrm{V_{CM}}(\ell)=\frac{\Phi(\vec{r}_1)+\Phi(\vec{r}_2)}{2}=-\frac{1}{\mu_0\epsilon_0 j\omega}\vec{\nabla}\cdot\left(\frac{\vec{\mathrm{A}}(\vec{r}_1)+\vec{\mathrm{A}}(\vec{r}_2)}{2}\right) \tag{18}$$

where

$$\vec{\mathrm{A}}(\vec{r}_1)+\vec{\mathrm{A}}(\vec{r}_2)\cong\frac{\mu_0}{4\pi}\frac{p\alpha}{2\pi}\vec{a}_z\int_0^{\mathcal{L}}\big(2g_3(\ell-\ell')-2g_2(\ell-\ell')\big)I_{\mathrm{CM}}(\ell')\mathrm{d}\ell' \tag{19}$$

Note that equation (19) is obtained by using all the approximations used above with the approximation $I_1(\ell')=I_2(\ell')\cong I_{\mathrm{CM}}(\ell')/2$. By making the same change of variable and inserting (19) into (18), the following equation is obtained

$$\frac{\partial}{\partial z}\int_0^{\mathcal{L}_z}\big(g_3(z-z')-g_2(z-z')\big)I_{\mathrm{CM}}(z')\mathrm{d}z'+j\omega 4\pi\epsilon_0\mathrm{V_{CM}}(z)=0 \tag{20}$$

which is also identical to the one derived for the one wire above ground shown in [8]. The CM current can be obtained by solving equations (17) and (20) by using the same method used in [8] and [13].

The scattered field radiated by the TWP and one wire above the ground are given by [13]

1) TWP scattered field

$$\vec{E}_{\mathrm{T}}^{\mathrm{sct}}=\vec{E}_{\mathrm{TWP}}^{\mathrm{sct}}+\vec{E}_{\mathrm{image}}^{\mathrm{sct}} \tag{20a}$$

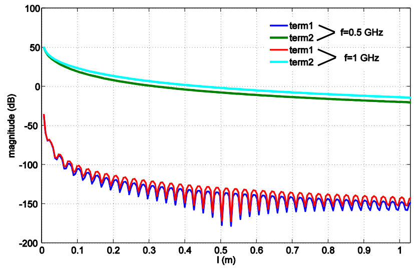

(a)

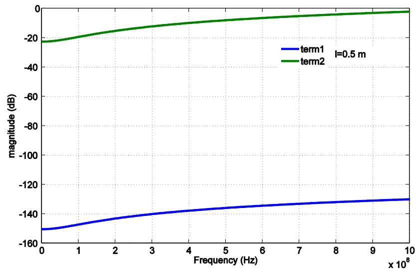

(b)

Fig. 4. The comparison between term 1 and term 2 shows that term1 is extremely small compared with term 2.

$$\vec{E}_{\mathrm{TWP}}^{\mathrm{sct}}=\frac{-j\eta_0 k}{4p\alpha}\int_0^{\mathcal{L}}\sum_{n=1}^{2}\left(1+\frac{1}{jkR_n}-\frac{1}{k^2R_n^2}\right)I_{\mathrm{CM}}(\ell')\vec{n}_{l_n}(\ell')\Psi(R_n)\,\mathrm{d}\ell'$$
$$-\frac{-j\eta_0 k}{4p\alpha}\int_0^{\mathcal{L}}\sum_{n=1}^{2}\left(1+\frac{3}{jkR_n}-\frac{3}{k^2R_n^2}\right)I_{\mathrm{CM}}(\ell')\big(\vec{n}_{l_n}(\ell')\cdot\vec{a}_{R_n}\big)\vec{a}_{R_n}\Psi(R_n)\,\mathrm{d}\ell' \tag{20b}$$

$$\vec{E}_{\mathrm{image}}^{\mathrm{sct}}=\frac{j\eta_0 k}{4p\alpha}\int_0^{\mathcal{L}}\sum_{n=1}^{2}\left(1+\frac{1}{jk\tilde{R}_n}-\frac{1}{k^2\tilde{R}_n^2}\right)I_{\mathrm{CM}}(\ell')\widetilde{\vec{n}_{l_n}}(\ell')\Psi(\tilde{R}_n)\,\mathrm{d}\ell'$$
$$-\frac{j\eta_0 k}{4p\alpha}\int_0^{\mathcal{L}}\sum_{n=1}^{2}\left(1+\frac{3}{jk\tilde{R}_n}-\frac{3}{k^2\tilde{R}_n^2}\right)I_{\mathrm{CM}}(\ell')\big(\widetilde{\vec{n}_{l_n}}(\ell')\cdot\vec{a}_{\tilde{R}_n}\big)\vec{a}_{\tilde{R}_n}\Psi(\tilde{R}_n)\,\mathrm{d}\ell' \tag{20c}$$

$$R_n=\|\vec{r}-\vec{r}_n'\|\quad,\quad\tilde{R}_n=\|\vec{r}-\tilde{\vec{r}}_n'\| \tag{20d}$$

$$\Psi(R)=\frac{\mathrm{e}^{-jkR}}{R} \tag{20e}$$

$$\vec{a}_{R_n}=\vec{R}_n/\|\vec{R}_n\|\quad,\quad\vec{a}_{\tilde{R}_n}=\widetilde{\vec{R}_n}/\left\|\widetilde{\vec{R}_n}\right\| \tag{20f}$$

2) One wire scattered field

$$\vec{E}^{\mathrm{sct}}=\vec{E}_{\mathrm{wire}}^{\mathrm{sct}}+\vec{E}_{\mathrm{image}}^{\mathrm{sct}} \tag{21a}$$

$$\vec{E}_{\mathrm{wire}}^{\mathrm{sct}}=\frac{-j\eta_0 k}{4\pi}\int_0^{\mathcal{L}_z}\left(1+\frac{1}{jkR_r}-\frac{1}{k^2R_r^2}\right)I_{\mathrm{CM}}(z')\vec{a}_z\Psi(R_r)\mathrm{d}z'$$
$$-\frac{-j\eta_0 k}{4\pi}\int_0^{\mathcal{L}_z}\left(1+\frac{3}{jkR_r}-\frac{3}{k^2R_r^2}\right)I_{\mathrm{CM}}(z')\big(\vec{a}_z\cdot\vec{a}_{R_r}\big)\vec{a}_{R_r}\Psi(R_r)\mathrm{d}z' \tag{21b}$$

$$\vec{E}_{\mathrm{image}}^{\mathrm{sct}}=\frac{j\eta_0 k}{4\pi}\int_0^{\mathcal{L}_z}\left(1+\frac{1}{jkR_i}-\frac{1}{k^2R_i^2}\right)I_{\mathrm{CM}}(z')\vec{a}_z\Psi(R_i)\mathrm{d}z'$$
$$-\frac{j\eta_0 k}{4\pi}\int_0^{\mathcal{L}_z}\left(1+\frac{3}{jkR_i}-\frac{3}{k^2R_i^2}\right)I_{\mathrm{CM}}(z')\big(\vec{a}_z\cdot\vec{a}_{R_i}\big)\vec{a}_{R_i}\Psi(R_i)\mathrm{d}z' \tag{21c}$$

$$R_r=\|\vec{R}_r\|=\|(x-h)\vec{a}_x+y\vec{a}_y+(z-z')\vec{a}_z\| \tag{21d}$$

$$R_i=\|\vec{R}_i\|=\|(x+h)\vec{a}_x+y\vec{a}_y+(z-z')\vec{a}_z\| \tag{21e}$$

$$\vec{a}_{R_r}=\vec{R}_r/\|\vec{R}_r\|\quad,\quad\vec{a}_{R_i}=\vec{R}_i/\|\vec{R}_i\| \tag{21f, g}$$

III. Validation of the CM Equivalent Circuit

In order to obtain the equivalent CM circuit of TWP, the following conditions should be satisfied:

(1) The CM current of TWP and the straight wire along the z-axis are the same.

(2) The scattered field produced by the TWP is equal to that of the straight wire outside the TWP.

In order to validate the accuracy of CM equivalent circuit, we perform a comparison between the results obtained by (20a) and (21a). The MoM result obtained by the commercial FEKO software is also presented for validation [14]. The parameters of

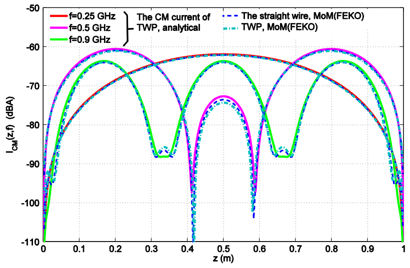

(a)

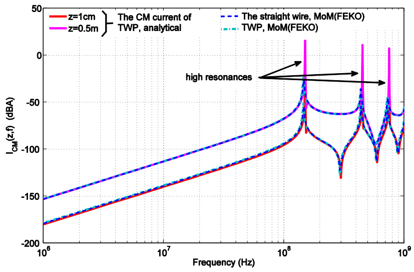

(b)

Fig. 5. The CM current magnitude induced along one wire and a TWP above the ground. (a) The CM current distribution. (b) The frequency response.

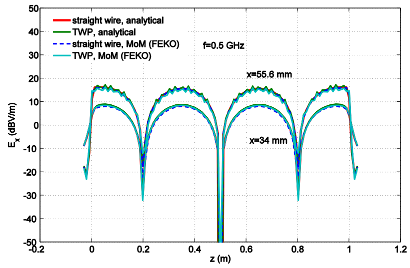

(a)

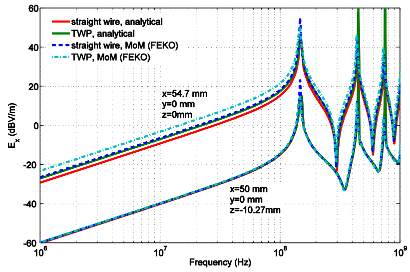

(b)

Fig. 6. The x-component of the near field radiations of one wire and a TWP above the ground. (a) The field distribution. (b) The field frequency response.

the TWP are chosen as $r_w = 0.5$ mm, $s = 4$ mm, $p = 5$ cm, $h = 5$ cm, and the TWP is extended along the z-axis with length $\mathcal{L}_z = 1$ m. The TWP and EM wave incidence are the same as both shown in Fig. 2, where a floating load $R = 100\ \Omega$ is connected to both terminals of the TWPs. It is worth noting that the floating load has no effect on the CM current along the TWP. Our numerical results are plotted in Figs. 5 and 6, and good agreements are obtained. This indicate that the CM equivalent circuit can be used to approximate both CM current and the near field of a TWP above a ground plane.

IV. Conclusion

In this paper, we have developed the integral equations of TWPs by using the scattered theory. The CM current along a TWP connected to floating terminals and also its near field have been predicted with very good accuracy. It has been shown that the antenna mode current along one wire above the ground is "identical" to the CM current generated by the TWPs above the ground. In addition, it has been proven that the CM equivalent circuit can be used to predict both CM current along a TWP and the corresponding near field.

Acknowledgement

This work was supported by the NSAF under Grant No. U1530121, the SAST2016059 of Shanghai Academy of Spaceflight Technology, the National Key Lab of Science and Technology on Electromagnetic Environment Effects, and the Science and Technology on Electronic Information Control Laboratory, in part by the National Natural Science Foundation of China under Grants 61822112.

References

[1] F. M. Tesche, M. V. Ianoz, and T. Karlsson, *EMC Analysis Methods and Computational Models*. New York: Wiely, 1997.

[2] C. R. Paul, *Analysis of Multiconductor Transmission Lines*. New York, NY: Wiley Interscience, 1994.

[3] S. Frangkel, *Quasi-TEM Transmission Line Theory*, Interaction Nate 135, Nov 1972.

[4] O. Gassab and W. Y. Yin, "Characterization of electromagnetic wave coupling with a twisted bundle of twisted wire pairs (TBTWPs) above a ground plane," *IEEE Trans. Electromagn. Compat.*, vol. 61, no. 1, pp. 251-260, Feb. 2019.

[5] O. Gassab and W. Y. Yin, "Efficient Characterization of Field-to-Wire Coupling in Twisted-Wire Pair with a Reference Wire," *International Symposium on Electromagnetic Compatibility (EMC EUROPE)*, Amsterdam, 2018, pp. 823-827.

[6] O. Gassab, L. Zhou, W. Y. Yin, and H. Xie, "Modelling electromagnetic wave coupling and mode conversion effects in multitwisted bundle of twisted-wire pairs (MTB-TWP) above ground plane", *Int. Journal Numer. Model.*, 2018, DOI:10.1002/jnm.2539.

[7] K. S. H. Lee, "Two parallel teminated conductors in external fields", *IEEE Trans. Electromagn. Compat*., vol. EMC-20, no. 2, May 1978.

[8] S. Tkatchenko, F. Rachidi, and M. Ianoz, "Electromagnetic field coupling to a line of finite length: theory and fast iterative solutions in frequency and time domains," *IEEE Trans. Electromagn. Compat.*, vol. 37, no. 4, pp. 509-518, Nov. 1995.

[9] J. B. Nitsch and S. V. Tkachenko, "Complex-valued transmission-line parameters and their relation to the radiation resistance," *IEEE Trans. Electromagn. Compat.*, vol. 46, no. 3, pp. 477-487, Aug. 2004.

[10] G. Lugrin, S. V. Tkachenko, F. Rachidi, M. Rubinstein, and R. Cherkaoui, "High-frequency electromagnetic coupling to multiconductor transmission lines of finite length," *IEEE Trans. Electromagn. Compat.*, vol. 57, no. 6, pp. 1714-1723, Dec. 2015.

[11] A. Vukicevic, F. Rachidi, M. Rubinstein, and S. V. Tkachenko, "On the evaluation of antenna-mode currents along transmission lines," *IEEE Trans. Electromagn. Compat.*, vol. 48, no. 4, pp. 693-700, Nov. 2006.

[12] K. Yuan, F. Grassi, G. Spadacini, and S. A. Pignari, "Reproducing field-to-wire coupling effects in twisted-wire pairs by crosstalk," *IEEE Trans. Electromagn. Compat.*, vol. 60, no. 4, pp. 991-1000, Aug. 2018.

[13] O. Gassab, L. Zhou, Z. G. Zhao, and W. Y. Yin, "Effect of the scattered field on the terminal risers in twisted-wire pairs with floating loads," *IEEE Trans. Electromagn. Compat.*, pp. 1-5., 2019. DOI: 10.1109/TEMC.2018.2888972.

[14] FEKO Suite 7.0 User's Manual. (May. 2014). © EM Software and Systems, S. A.(Pty) Ltd., Stellenbosch, South Africa [Online]. Available: www.feko.info.